Available online at www.sciencedirect.com
SCIENCE DIRECT®
Composites: Part A 34 (2003) 1143–1149
composites
Part A: applied science and manufacturing
www.elsevier.com/locate/compositesa

Microstructure and chemical analysis of C/Cu/Al interfacial zones

J.F. Silvain[a], A. Proult[b], M. Lahaye[a], J. Douin[c,*]

[a]Institut de Chimie et de la Matière Condensée de Bordeaux, 87 Av. Dr A. Schweitzer, 33608 Pessac cedex, France
[b]Laboratoire de Métallurgie Physique, Boulevard 3, Teleport 2, BP 179, 86960 Futuroscope cedex, France
[c]Laboratoire d'Etude des Microstructures (UMR 104), CNRS/ONERA, BP 72, 29, Avenue De La Division Leclerc, 92322 Châtillon cedex, France

Received 10 March 2003; revised 25 July 2003; accepted 21 August 2003

Abstract

The fibre–matrix interface in carbon–aluminium composites has been examined. Composites were prepared using uncoated carbon preforms and carbon preforms coated with copper. Auger and transmission electron microprobe microscopy were used to study the interface. The role of the copper layer on the microstructural and chemical evolution of the system after a 96 h heat treatment at 600 °C is discussed.

Keywords: A. Metal–matrix composites (MMCs); A. Carbon fibre; B. Microstructure; D. Chemical analysis

1. Introduction

Graphite/aluminium composites are promising composites for structural applications due to their high specific properties (see for example Ref. [1]). However, the elaboration of such composites by infiltration of molten aluminium into carbon fibre preforms undergoes three major difficulties: (1) a lack of wetting of the fibre with the molten aluminium, (2) a deterioration of the fibre properties during composite processing, and (3) the formation of brittle reaction products between the fibre and the matrix.

To overcome these difficulties, coatings can be deposited on fibres by various methods such as electroless deposition, electroplating, vapour deposition and plasma spraying [2]. In particular, it has been shown that metallic coatings deposited on carbon fibres helps the infiltration by the molten aluminium of unidirectional performs, resulting in a decrease of applied squeeze casting pressures [3].

However, because most metal–matrix composites (MMC) can be regarded as non-equilibrium systems during their preparation and their high temperature service, a gradient of chemical potential exists at the fibre/matrix (F/M) as well as at the fibre/coating/matrix interfaces. This difference in chemical potential provides the driving force for diffusion and/or chemical reaction when the composites are heated to elevated temperatures [4].

Also, residual thermal stresses in MMCs result, during cooling, either from temperature gradients within the specimen or from a difference of coefficient of thermal expansion (CTE) between the constituents. The former effect can be controlled by a slow cooling rate. However, this slow cooling rate is in contradiction with the high cooling rate which is usually applied during MMC fabrication. In fact, a high cooling rate is most of the time required to minimise the F/M interfacial reaction zone and to reduce grain growth within polycrystalline reinforcement [5–7]. Unless the CTEs of the constituents are identical or unless adaptive coatings are deposited on fibres in order to adjust CTE mismatch, MMC processing will thus always give rise to interfacial induced stresses. Usually, the larger contraction of the matrix compared to the reinforcement leads to tensile residual stresses in the matrix and to compressive residual stresses in the reinforcement. Since the fibres are always fragile, deformation must occur in the matrix in order to accommodate the CTE stresses during the processing. Thus the choice of the coating is of prime importance in order to prevent cracks initiation and growth. Notice that, in certain circumstances, while the thermal induced stresses are very high, no crack in the composite is observed, even for a fragile matrix [8]. In such cases, the induced deformation must be accommodated somehow, either in the fibre or in the matrix.

Gold, nickel and copper are the three main surface coatings used for carbon fibres in MMCs. They are chemically stable with carbon and can be deposited by

* Corresponding author. Tel.: +33-1-46-734442; fax: +33-1-46-734155.
E-mail address: douin@onera.fr (J. Douin).

1359-835X/$ - see front matter © 2003 Elsevier Ltd. All rights reserved.
doi:10.1016/j.compositesa.2003.08.006

electrochemical, chemical or physical methods. It has been shown that gold and nickel coatings reduce the formation of undesirable Al_4C_3 compound at F/M interfaces after different heat treatments [9–11], but no investigation has been performed on the other possible metallic coating, i.e. copper. So, in order to consider its use in C/Al composites, the interfacial reactions occurring at the C/Cu/Al interface compared with C/Al interface and the microstructural evolution at the interface, that is the characterisation of the interfacial dislocations which are induced during cooling in order to accommodate the stresses in the F/M zone close to the matrix, were studied in non-annealed and annealed composites. The composition of the phases formed at the interface, under controlled conditions, were analysed using Auger electron spectroscopy (AES) line scan profiles. The weak beam dark field microscopy technique was used to determine the Burgers vectors, lines and gliding planes of the different families of dislocations present in the vicinity of the F/M interface.

2. Experimental

2.1. Preparation of composites

Composites were obtained by a squeeze casting process which is one of the most important casting methods presently used [12,13]. The matrix was pure aluminium. The carbon preforms consisted of either uncoated or coated T700 fibres with a 10 μm diameter. The copper coating was realised according to an electrochemical technique which is essentially based on the dipping of the fibre preforms in three successive baths: sensitisation, activation and coating [14]. The first two steps took place at ambient temperature while the third one was realised at 65 °C. The chosen experimental conditions allowed a dense 0.5 μm copper film to be deposited on the carbon fibres. The Al liquid matrix at 800 °C was poured into the preform which was preheated at 450 °C; this procedure was carried out in an ambient atmosphere. The pressures applied to the system were up to 100 MPa. After cooling, ingots with approximate dimensions of $70 \times 40 \times 40$ mm^3 were obtained. They were cut using a diamond saw and subsequently polished to a mirror finish for AES observations.

2.2. Analysis methods

2.2.1. Auger electron spectroscopy and mathematical line scan treatment

Quantitative surface analysis is non-trivial and surface chemical composition determination via AES may be handicapped by several factors such as matrix effects, electron escape depth, analyser transmission function, etc.

To perform such a calculation, peaks from the specimens and standards have been collected in the direct, N(E), mode. We have, for background subtraction, use the background devised by Shirley [15], which rises in proportion to the area of peak at higher energies above the background. However, we cannot directly use the areas for the quantitative calculations, and it is necessary to consider various electron/matter interaction phenomena such as matrix effect and interaction cross section. These corrections are integrated in a single factor called sensitivity factor given directly by the Thermo VG Scientific program for single element or calculated with standard for multi-element materials. Using these collected mode, background subtraction and sensitivity factor the accuracy of the atomic concentration measured is around 5%.

The AES data were acquired on a VG-MICROLAB 310-F Microprobe with a lateral resolution of 20 nm. Analyses conditions were an accelerated voltage and beam current of 10 keV and 1 nA, respectively. The data were recorded in the conventional EN(E) mode. The energy range investigated in this multiplexing technique were the following for each element: O, 495–515; Al, 1375–1405; Cu, 900–930 and C, 250–275 eV. The peak identification was performed by reference to an AES database [16] or from reference compounds analysed in the same apparatus. In many cases, peak overlap or small changes in chemistry make the chemical analysis of a multi-component mixture difficult. So, a specific procedure was followed to analyse a set of spectra obtained by line profiles in order to plot the atomic concentration of each element versus the point position in the line, in respect to its chemical state. Data acquired at different position across the sample are computer-analysed using numerical methods applied to the matrix data. Non-linear least square fitting (NLLSF) was the well-known technique used during this work.

2.2.2. Sample preparations for TEM observations

Thin slides were cut at a 90° angle with respect to the fibres axis and thinned by mechanical grinding to approximately 50 μm. Further thinning followed with an ion miller using a collimated beam of argon ions accelerated by a voltage of 6 kV at liquid N_2 temperature. These thin slides were examined by conventional and weak beam transmission electron microscopy (TEM) in a JEOL 200 CX microscope operating at 200 kV.

3. Results and discussion

3.1. Fibre/matrix interface analysis in Al/C composites

Fig. 1 shows an AES line scan profile across the interface of a non-annealed C/Al composite (reference sample). Three regions can be observed: (i) on the left side of the figure, the aluminium matrix, (ii) in the middle part, an interface zone where carbon, aluminium and oxygen are present and (iii) on the right side, the carbon substrate. The intersection of the 20% atomic concentration (AC) and the 80% AC with the carbon concentration curve gives

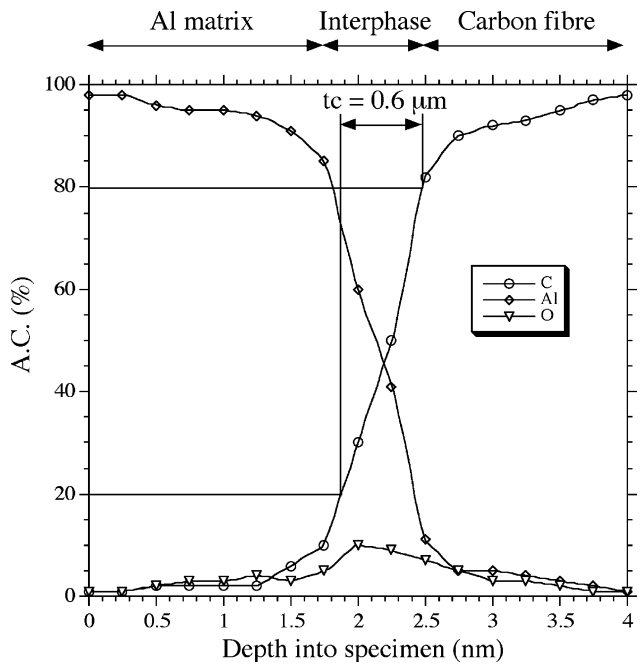

Fig. 1. AES line scan profile across the F/M interface for an as-fabricated Al/C composite.

an estimate of the thickness of the carbon reaction zone. The evolution of this thickness (t_c) with the annealing time and the presence or not of the copper coating is given in Table 1.

Fig. 2 shows the same type of interface after a long thermal treatment (600 °C for 96 h). Aluminium matrix and carbon substrate are still present on the sides of the figure, but now the interface zone is modified as shown by the changes of the atomic concentrations of Al and C in the vicinity of the interface.

It has to be mentioned that the oxygen content does not increase with annealing time and temperature and therefore the influence of this species is not considered in the following. The change of the interface zone is attributed to the formation of Al_4C_3 that results from the dissolution of carbon and its subsequent diffusion into the aluminium matrix. The thickness of the carbon reaction zone is approximately three times larger after annealing (cf. Table 1) and can be correlated with a roughening of the fibre surface as observed by scanning electron microscopy.

3.2. Fibre/matrix interface analysis in C/Cu/Al composites

As a general concern, the formation of Al_4C_3 must be prevented, first because it is associated with degradation and

Table 1
Annealing conditions for the different composites

Annealing conditions	Al/C	Al/C annealed	Al/Cu/C	Al/Cu/C annealed
t_c	0.6	1.5	1	0.8
T (°C)	0	600	0	600
Time (h)	0	96	0	96

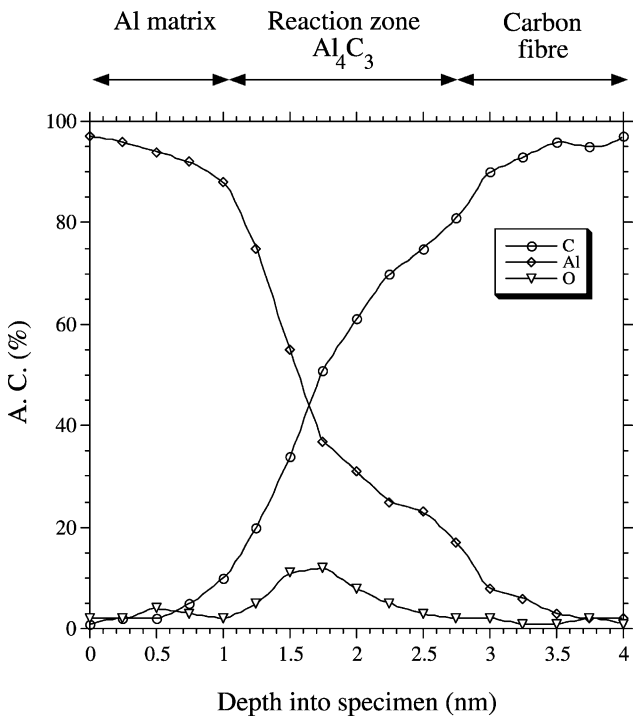

Fig. 2. AES line scan profile across the F/M interface for an Al/C composite, annealed at 600 °C for 96 h.

a decrease of the diameter of the carbon fibre and second because of the fragile nature of Al_4C_3.

Fig. 3 shows an AES line scan profile across the F/M interface for an non-annealed C/Cu/Al composite, that is as obtained by the squeeze casting process. In fact, the length of the performed scan (4.1 μm) allowed us to analyse

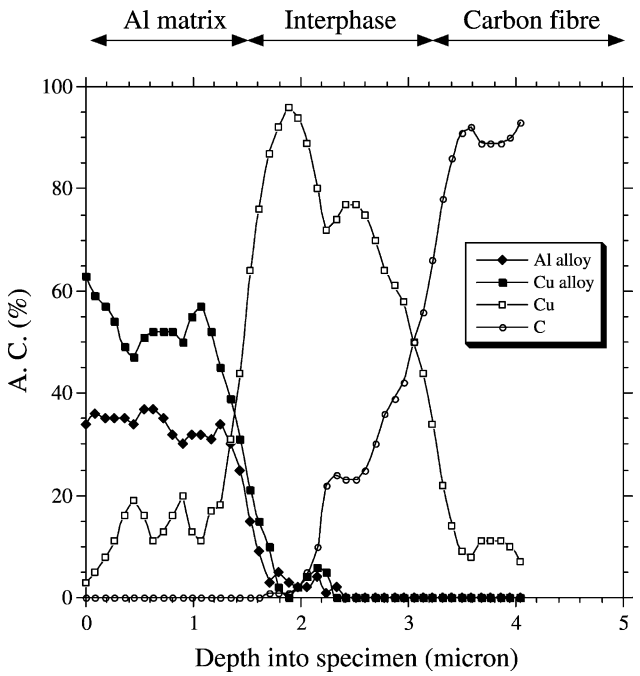

Fig. 3. AES line scan profile across the F/M interface for an as-fabricated Al/Cu/C composite.

the aluminium matrix, the copper layer (approximately 2 μm thick) and the carbon fibre. Three regions can be observed: (i) on the right side, the carbon fibre containing a small concentration of metallic copper, (ii) in the middle a narrow interface zone constituted of carbon and copper and (iii) on the left side Cu alloy and Al alloy with a small concentration of Cu metal. Out of scale on the left side, the Al matrix is present and only constituted of pure aluminium. The numerical NLLSF treatment indicates the presence of aluminium and carbon species on the middle area, and, on the left side, two types of copper species (Cu metal and Cu alloy) and one type of aluminium species (Al alloy). The small value of t_c (cf. Table 1) and the absence of Al and C alloy give evidence of the non-formation of carbide. Consequently, the sacrificial copper layer actually prevented the formation of Al_4C_3. The copper layer does not act directly as a diffusion barrier against carbon but leads to the formation of a stable Al–Cu intermetallic compound by diffusion of copper in the aluminium matrix during elaboration process.

The evolution of the C/Cu/Al interface was investigated after composite annealing at 600 °C during 96 h. Fig. 4 presents a SEM image of a section of an annealed composite and the corresponding AES line profile for the L1 line is presented in Fig. 5. Notice that the three scans line profile (L1, L2 and L3) give similar results and evidence the good homogeneity of the copper coating all around each carbon fibre. The diameters of the carbon fibres have not been modified by the thermal treatment and no degradation can be observed by SEM analyses. However, the interphase zone is much more complex than for the non-annealed C/Cu/Al composite. Indeed, the NLLSF treatment showed the presence of a small amount of Al alloy at the interphase area, attributed to Al_4C_3 carbide, and of Al–Cu intermetallic. As for the non-annealed composite, Cu diffuses inside the Al matrix to form a Cu(rich)–Al compound ((1) in Fig. 5) close to the Al matrix, a Al(rich)–Cu compound ((3) in Fig. 5) close to the C fibre. Between these two

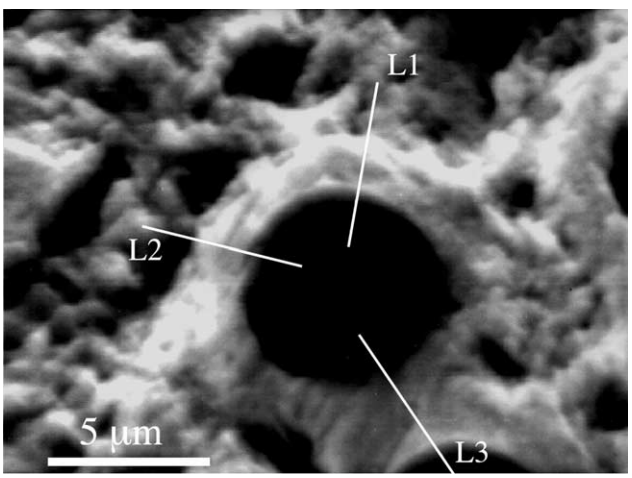

Fig. 4. SEM micrograph showing the AES line profiles and the shape of the carbon fibre after annealing.

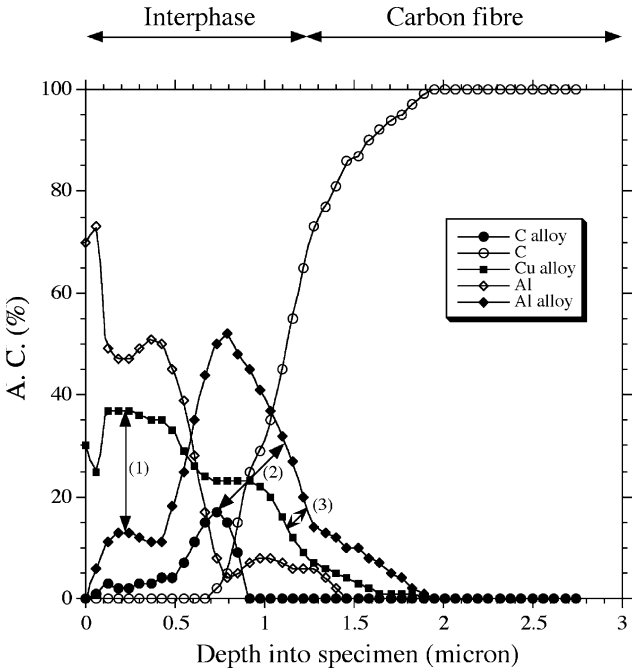

Fig. 5. AES line scan profile across the F/M interface for an Al/Cu/C composite, annealed at 600 °C for 96 h. (1): $CuAl_2$, (2) Al_4C_3, (3) Cu_9Al_4.

compounds, the formation of the Al_4C_3 carbide can be observed ((2) in Fig. 5). The formation of Al(rich)–Cu compound ($CuAl_2$) which can subsequently react with copper to form a Cu(rich)–Al compound (Cu_9Al_4), a reaction controlled by interfacial and grain boundary diffusion, has already been reported for annealed Cu/Al thin films [17].

3.3. TEM investigation on C/Cu/Al annealed composites

3.3.1. Interface analysis

C/Cu/Al composites annealed at 600 °C have been investigated by TEM. Fig. 6 shows a TEM low magnificated micrography obtained with an electron beam parallel to the fibre axis. The carbon fibres appear undamaged, no

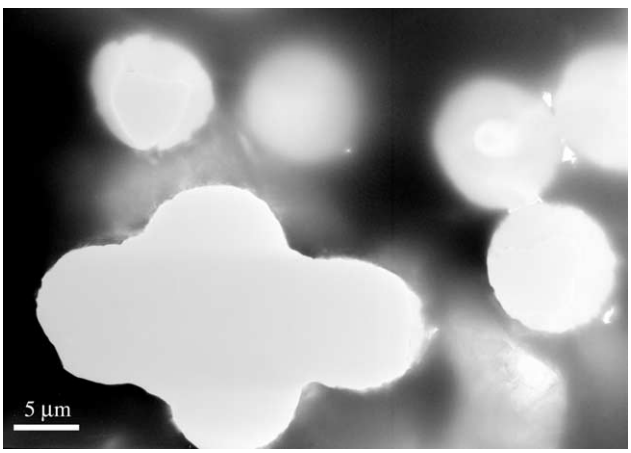

Fig. 6. Low magnificated TEM micrograph of AlCu/C annealed composite. The carbon fibres appear undamaged.

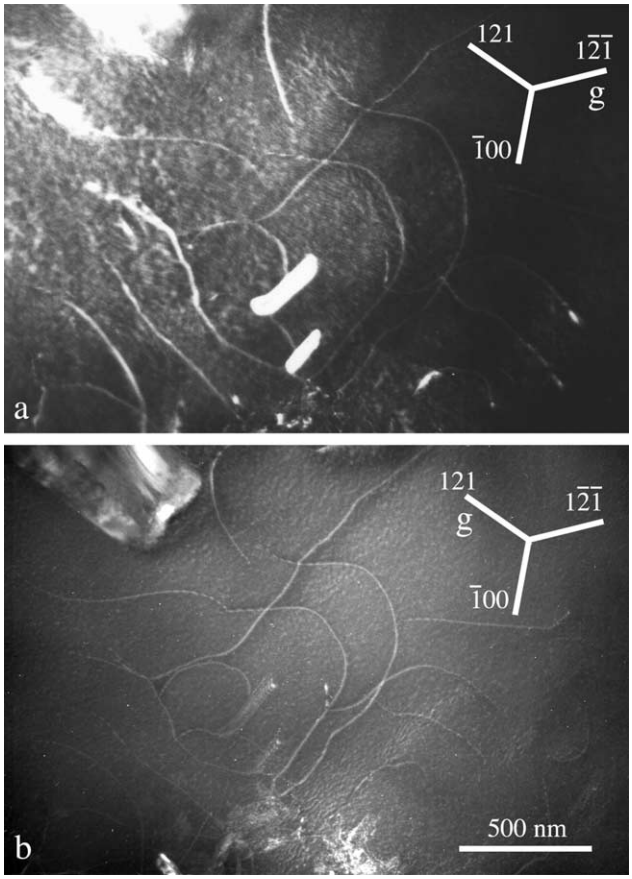

Fig. 7. Interface in AlCu/C annealed composite (weak-beam image). (a) Diffracting condition: $\mathbf{g} = 1\bar{2}\bar{1}$; platelets of Al_4C_3 are visible with a strong bright contrast; (b) $\mathbf{g} = 121$. The dislocations are lying in the (001) plane of Al_2Cu, their Burger vector is $\mathbf{b} = [001]$.

deterioration have occurred during the composites processing.

Around the carbon fibres (cf. Fig. 7), large platelets are observed whose diffraction patterns are consistent with the Al_4C_3 structure (see for example Fig. 8). Between fibres, an Al–Cu intermetallic is formed containing dislocations and small precipitates. The diffraction patterns of the AlCu intermetallic correspond to the Al_2Cu structure (Fig. 9). This phase is the phase called Θ in the precipitation sequence of Guinier–Preston zones $\Theta'' \rightarrow \Theta' \rightarrow \Theta$ occurring during ageing of α-AlCu solid solution. Small precipitates observed in Al_2Cu could correspond to the Al_4Cu_9 compound. RX analysis in the microscope confirmed a composition close to the matrix Al_2Cu but, because of the small size of the precipitates, it did not allow for the complete determination of the composition.

3.3.2. Dislocation microstructure

Residual thermal stresses in MMC result from the difference in CTE of the fibre and the surrounding matrix, the accumulation of stress being also enhanced by the high cooling rate during formation of the composite. In order to avoid cracks formations at or near the interface, this stress

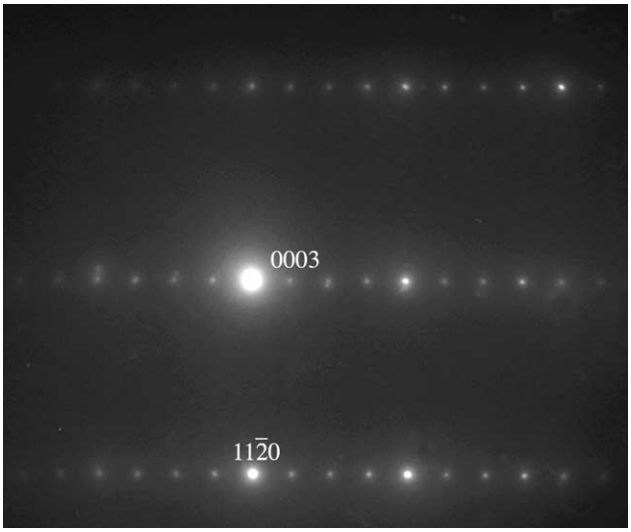

Fig. 8. Example of a characteristic diffraction pattern from the platelet with Al_4C_3 structure. This rhombohedral $R\bar{3}2/m$ structure can also be described as an hexagonal structure with parameters $a = 0.3325$ and $c = 2.494$ nm and the hexagonal notation has been used to index the diffraction pattern here.

must be accommodated somehow. It has been previously shown in the Al_2O_3/NiAl composite [8] that the residual stress can be accommodated by nucleation of dislocations in the matrix with the right Burgers vector and the required orientation. As the accommodation is best handled in the close vicinity of the interface, we will study here the microstructural properties of the material at the contact of and surrounding the fibres, i.e. Al_2Cu.

On the basis of simple elasticity (see for example Ref. [18]), three type of residual stress are expected in a matrix surrounding a fibre, namely longitudinal, hoop and radial stresses. As the radial stress is continuous through the interface, that is, it is the same for the fibre and the matrix at the interface, there is no need of interfacial dislocations to accommodate the radial stress. One important result of our observations to point out is the fact that a preferential growth direction of Al_2Cu relative to the fibre axis exists. Indeed, the [001] direction (or c direction) of the Al_2Cu structure (Fig. 9) has been repeatedly found parallel to

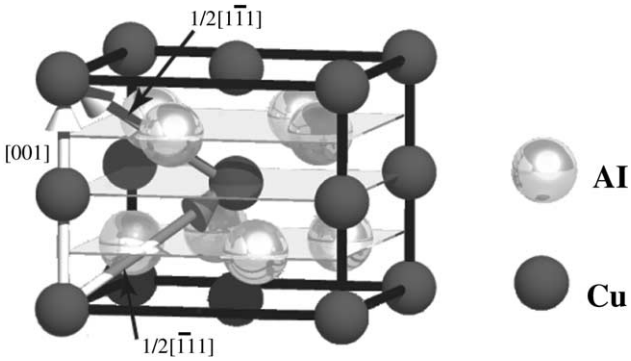

Fig. 9. Structure of Al_2Cu. Spatial group I4/mcm, $a = 0.6052$, $c = 0.4878$ nm.

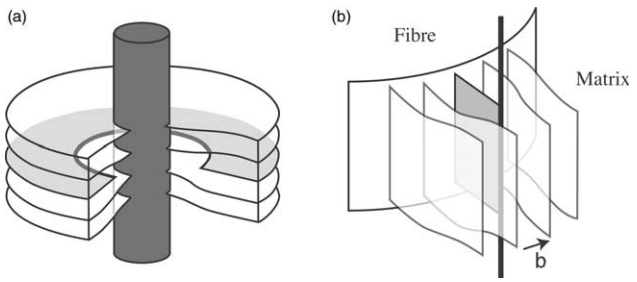

Fig. 10. Accommodation of the residual stress resulting from cooling during composite elaboration in the case of a fibre's CTE smaller than the matrix's CTE (after Douin et al. [20]). (a) Accommodation of the axial stress by insertion of edge dislocations around the fibre; (b) accommodation of the hoop stress by insertion of edge dislocations parallel to the fibre.

the carbon fibre axis. It is worth pointing out that Al_2Cu is extremely brittle up to 750 K and does not develop appreciable plasticity below 800 K [19]. However, observations show no crack in the vicinity of the fibre, and a non-negligible density of pure edge dislocations with a Burgers vector [001] lying in the (001) plane perpendicular to the fibre axis (Fig. 8). Notice that [001] is the shortest perfect translation of the Al_2Cu structure, and, as such, is favoured to be the Burgers vector of the easiest activated dislocations. As these dislocations simply lead to the insertion of half-planes around the fibre axis (Fig. 10a), they best accommodate the longitudinal stress.

Accommodation of hoop stress needs dislocations with a Burgers vector with a non-zero component perpendicular to the fibre (Fig. 10b). The fibres being aligned along the [001] axis of Al_2Cu, no hoop stress can be accommodated by dislocations with a [001] Burgers vectors. Thus, accommodation should be attained by activation of others dislocations, the best being edge dislocations parallel to the fibre axis. Dislocations with $1/2\langle 111\rangle$ Burgers vector, which is the second shortest perfect translation of the Al_2Cu structure (Fig. 9), have been observed but usually the interactions between the different $1/2\langle 111\rangle$ dislocations and the [001] dislocations result in a complicated network, as exemplified in Fig. 11. As it does not contain the Burgers vectors of the $1/2\langle 111\rangle$ dislocations, the plane of the network is not a glide plane of these $1/2\langle 111\rangle$ dislocations. It also does not contain the fibre axis. However, a more careful examination indicates that such networks result from a compromise between the best hoop stress accommodation, which would appear in a plane containing the fibre direction, and the reduction of the total energy of the configuration, that is in a plane which minimises the total energy of the network.

Finally, we would like to emphasize on the role of stress accommodation during solidification and growth of the material surrounding the fibre. As the longitudinal stress appears to have an especially important role for long and thin fibres, it is believed that longitudinal stress accommodation could be a strong driving force during solidification. The surrounding matrix would choose an orientation relationship with the fibre which minimizes the final accumulated longitudinal stress. This promotes the directions of growth for which the easiest activated dislocation nucleation best accommodate this residual stress. As a hint for the validity of 'accommodation-induced growth', we recall that such

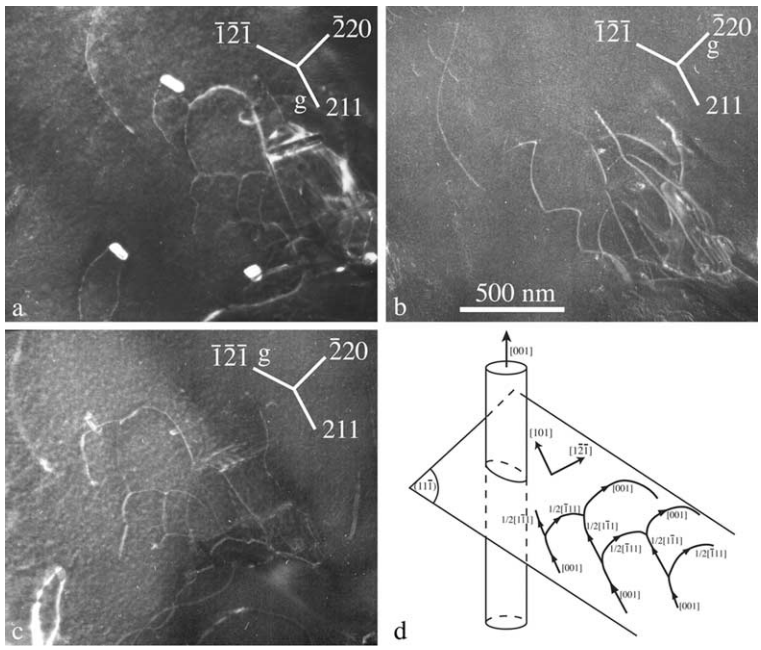

Fig. 11. Network of dislocations in Al_2Cu resulting from the interactions between $1/2\langle 111\rangle$ dislocations and the [001] dislocations. (a) $\mathbf{g} = 211$; (b) $\mathbf{g} = \bar{2}20$; (c) $\mathbf{g} = \bar{1}2\bar{1}$; (d) schematic of the configuration. Notice that the plane of the network is not a glide plane of the involved $1/2\langle 111\rangle$ dislocations, and does not contain the fibre axis. Thus, this network appears to result from a compromise between a best hoop stress accommodation and the reduction of the total energy of the configuration.

orientation relationships were repeatedly found here for Al_2Cu around C fibres (direction of growth [001]) as well as for NiAl around Al_2O_3 fibres [8] (direction of growth: [110]).

4. Conclusions

The nature of fibre/matrix interfaces existing in Al/C composites was investigated depending on the presence of a copper interlayer deposited on carbon fibres. It has been shown that the sacrificial copper layer prevents the formation of Al_4C_3 by formation of a stable Al_2Cu intermetallic compound. Even if this compound is known to be fragile up to 800 K, sufficient plasticity is activated for the accommodation of the residual stresses created during formation of the composite, leading to a crack-free material.

References

[1] Rocher JP, Quenisset JM, Naslain R. J Mater Sci Lett 1985;4:1527.
[2] Honjo K, Shindo A. J Mater Sci 1986;21:2043.
[3] Chou TW, Kelly A, Okura A. Composites A 1985;7:201.
[4] Nourbakhsh S, Margolin H. Metall Trans A 1991;22A:3059.
[5] Silvain JF, Bihr JC, Le Petitcorps Y, Lahaye M. Adv Sci Technol 1994;7:719.
[6] Jeng SM, Yang JM, Amato RA. MRS Symp Proc 1992;273:547.
[7] Silvain JF, Le Petitcorps Y, Albingre L. Rev Met 1994;9:1348.
[8] Silvain JF, Bihr JC, Douin J. Composites A 1998;29:1175–83.
[9] Silvain JF, Turner MR, Lahaye M. Composites A 1996;27:691.
[10] Silvain JF, Le Petitcorps Y, Lahaye M, Turner M. Surf Sci 1996; 352–354:839–44.
[11] Silvain JF, Heinz JM, Lahaye M. J Mater Sci 2000;35:961–5.
[12] Abi Y, Horikiri S, Fujimura K, Ichiki E. In: Hayashi T, editor. Proceedings of the ICCM-IV. ; 1982. p. 1427.
[13] Clyne TW, Mason JF. Metall Trans A 1987;18:1519.
[14] Silvain JF, Chazelas J, Trombert S. Appl Surf Sci 2000;153:211.
[15] Shirley DA. Phys Rev B 1972;5:4709.
[16] Handbook of Auger electron spectroscopy. Davis LE, Mac Donald NC, Palmberg PW, Riach GE, Weber RE (eds.), Eden Prairie, USA: Physical Electronic Publisher; 1979.
[17] Jiang HG, Dai JY, Tong HY, Ding BZ, Song QH, Hu ZQ. J Appl Phys 1993;74(10):6165.
[18] Warwick CM, Clyne TW. J Mater Sci 1991;26:3817–27.
[19] Mondolfo LF. Aluminum alloys: structure and properties. Boston: Butterworths; 1979. p. 254.
[20] Douin J, Donnadieu P, Finel A, Dirras GF, Silvain JF. Composites A 2002;3:1397–1401.